A murine photothrombotic stroke model with an increased fibrin content and improved responses to tPA-lytic treatment

Yu-Yo Sun,[1,*] Yi-Min Kuo,[1,2,*] Hong-Ru Chen,[1] Jonah C. Short-Miller,[1] Marchelle R. Smucker,[1] and Chia-Yi Kuan[1]

[1]Department of Neuroscience, Center for Brain Immunology and Glia, University of Virginia School of Medicine, Charlottesville, VA; and [2]Department of Anesthesiology, Taipei Veterans General Hospital and National Yang-Ming University School of Medicine, Taipei, Taiwan

Key Points

- Adding low-dose thrombin into photothrombosis elevates the fibrin content in blood clots.

- This modified photothrombosis model has greatly improved responses to tPA-lytic treatment.

The Rose Bengal (RB) dye-based photothrombotic stroke (PTS) model has many methodological advantages including consistent location and size of infarct, low mortality, and relatively simple surgical procedures. However, the standard PTS has the caveat of poor responses to tissue-type plasminogen activator (tPA)–mediated lytic treatment, likely as a result of the platelet-rich, fibrin-poor content of the blood clots. Here we tested whether the admixture of thrombin (80 U/kg) and RB dye (50 mg/kg) in the proximal middle cerebral artery (MCA)–targeted PTS will modify the clot composition and elevate the responsiveness to tPA-lytic treatment (Alteplase, 10 mg/kg). Indeed, intravital imaging, immunostaining, and immunoblot analyses showed less-compacted platelet aggregates with a higher fibrin content in the modified thrombin (T) plus RB photothrombotic stroke (T+RB-PTS) model compared with the standard RB-PTS-induced clots. Both RB-PTS and T+RB-PTS showed steady recovery of cerebral blood flow (CBF) in the ischemic border from 1 day after infarction, but without recanalization of the proximal MCA branch. Intravital imaging showed high potency of restoring the blood flow by tPA after single vessel-targeted T+RB-PTS. Further, although intravenous tPA failed to restore CBF or attenuate infarction in RB-PTS, it conferred 25% recovery of CBF and 55% reduction of the infarct size in T+RB-PTS ($P < .05$) if tPA was administered within 2 hours postphotoactivation. These results suggest that T+RB-PTS produces mixed platelet:fibrin clots closer to the clinical thrombus composition and enhanced the sensitivity to tPA-lytic treatment. As such, the modified photothrombosis may be a useful tool to develop more effective thrombolytic therapies of cerebral ischemia.

Introduction

The search for acute stroke therapies requires multiple preclinical models to address different aspects of the pathological mechanisms. The photodynamic dye (eg, Rose Bengal [RB])–based photothrombotic stroke (PTS) model has many strengths, including consistent location and size of infarct, relatively simple surgical procedures, and a low mortality rate of animals.[1-4] The introduction of middle cerebral artery (MCA)–targeted photoactivation (as opposed to aiming the laser beam at a large brain area) further widened the ischemic penumbra to study peri-infarct neovascularization.[5] Yet RB-based photothrombosis largely remains a model of permanent ischemia, as it is resistant to the tissue-type plasminogen activator (tPA)–lytic treatment.[3,4,6] The poor responses to tPA have prevented the application of RB photothrombosis for studying the pathology of transient ischemia and the search for better thrombolytic therapies.

The root cause of RB photothrombosis' poor responses to tPA-lytic therapy may be its low fibrin content in compacted platelet aggregates as the blood clots.[2] As the recent advances of endovascular stroke therapies have enabled the histological analysis of acute clinical thrombi, it became clear that the

The full-text version of this article contains a data supplement.
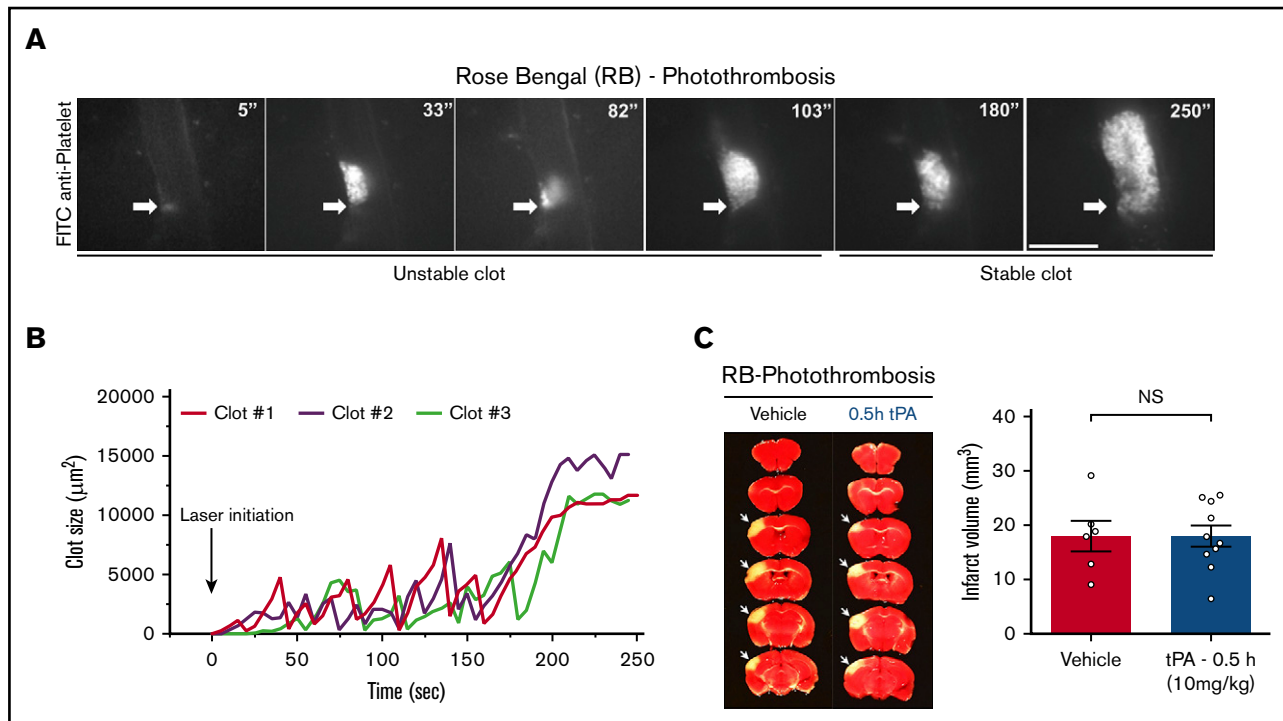
Figure 1. The RB photothrombotic stroke model induces platelet aggregates and responds to tPA-lytic treatment poorly. (A) Single vessel-directed RB photothrombosis induced a train of initially unstable platelet clots that transformed into rapidly expanding platelet aggregates, as shown by intravital microscopy using DyLight488-conjugated anti-GPIbβ antibody (arrow indicates the site of 20-μm diameter laser photoactivation; also see supplemental Video 1). Scale bar, 50 μm. (B) Tracing of the size of 3 photoactivation-induced platelet aggregates under single-vessel RB-PTS over time. The initial platelet clots were repeatedly flushed away by the blood flow until the later clot adhered to the endothelial wall and expanded in size rapidly (n = 3). (C) Intravenous application of 10 mg/kg tPA at 30 minutes after the proximal MCA branch-directed RB-PTS failed to reduce the infarct size. The TTC-unstained infarcted area (indicated by arrows) was 18 ± 1.95 mm^3 in tPA-treated mice (n = 10) and 18 ± 2.80 mm^3 in the vehicle-treated mice (n = 6) at 24 hours recovery. $P > .05$ by unpaired Student t test. Shown are the mean $\pm$ standard error of the mean. NS, not significant.

majority are composed of random fibrin:platelet deposits interspersed with leukocytes and confined erythrocyte-rich regions.[7,8] Compared with the clinical thrombi, neither the RB- nor ferric chloride ($FeCl_3$)–induced blood clots produce a substantial amount of fibrin, which rationalizes its resistance to tPA-lytic treatment.[9,10] In contrast, in situ microinjection of thrombin into the proximal MCA branch produces thrombi composed mainly of polymerized fibrin with a few cells and platelets.[11] The in situ thrombin microinjection stroke model is highly sensitive to tPA-lytic treatment, but its low platelet content also deviates from the norm of clinical thrombi and may limit its responsiveness to the antiplatelet agents in adjuvant thrombolysis.[11-14]

Given these considerations, we decided to examine whether intravenous injection of a mixture of thrombin and RB for the proximal MCA branch-targeted photoactivation (T+RB-PTS) will elevate the fibrin content in the induced thrombi, as well as the responsiveness to tPA- lytic treatment, compared with the standard RB-PTS model. Our results support both predictions and suggest that the modified photothrombosis model may be a useful tool to study thrombolysis and therapeutically enhanced collateral circulation.[14-18]
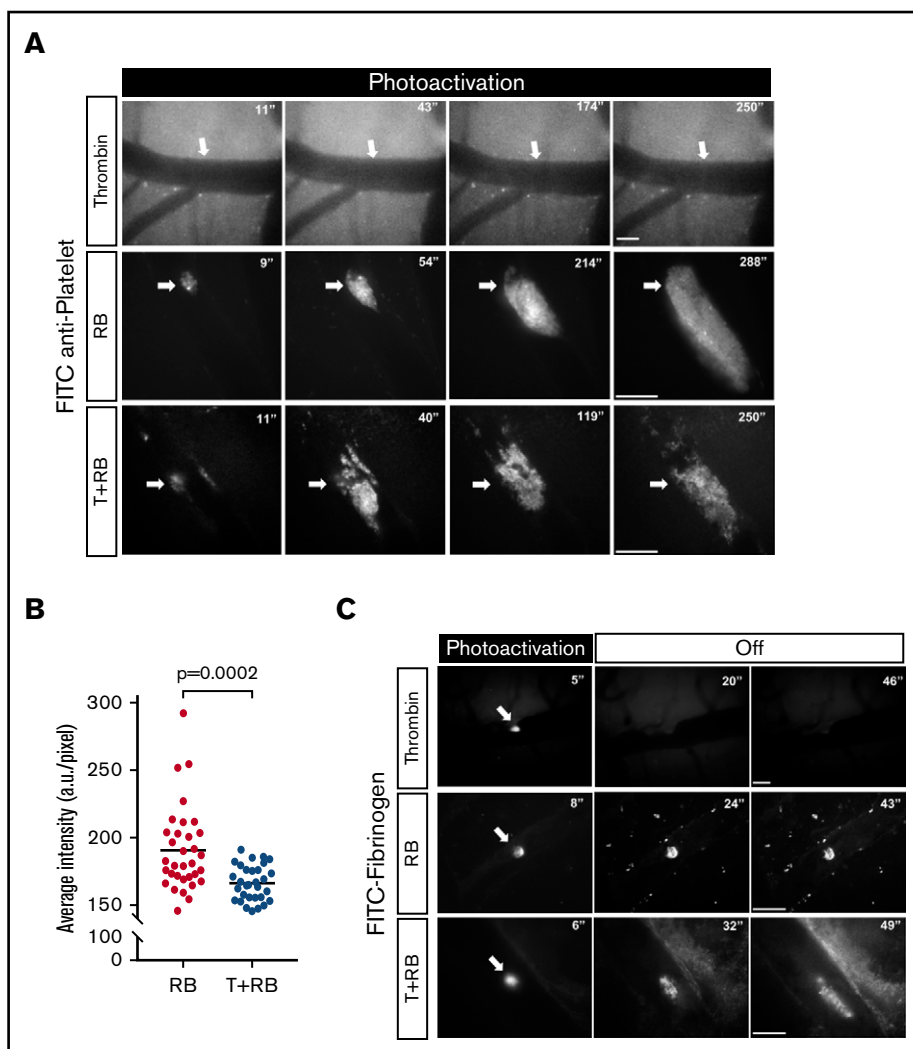
Methods

Stroke surgery

Ten- to 12-week-old male C57BL/6 mice were subjected to RB- or T+RB photothrombosis at the proximal MCA branch, as described.[1,2]

The mouse was anesthetized when the temporal muscles were divided, and a 1-mm-diameter spot was drilled-thinned in the skull over the proximal MCA branch. Next, 50 mg/kg RB (Sigma) or the RB and bovine thrombin (80 U/kg; Sigma) mixture was injected into the retro-orbital sinus, and the window was illuminated by a 543-nm laser beam (5 mW) ~1 mm in diameter for 20 minutes. The ipsilateral common carotid artery was ligated to decrease collateral perfusion and variations of the infarct size and for 7-day monitoring of cerebral blood flow (Figure 5) and for tPA-lytic treatment (Figures 1 and 7). Mice were randomized for treatments (10 mg/kg Alteplase, 50% injected as a bolus and 50% infused over the course of 30 minutes through tail vein, as previously described[19]), and the infarct size was analyzed using triphenyl tetrazolium chloride (TTC) stain at 24 hours recovery by investigators who were blinded to the treatment. Mouse brains were sectioned to 1-mm-thick slices, and the TTC-unstained volume in all sections was quantified and added using the NIH ImageJ software. Two outliers (mean $\pm$ >2 SD) were excluded in the experiment of tPA-mediated thrombolytic treatment (Figure 7). All procedures were approved by the Institutional Animal Care and Use Committee at the University of Virginia.

Intravital microscopy

Real-time thrombus formation was visualized on a spinning-disc confocal microscope (Visual Dynamix). Briefly, the craniotomy of 3 to 5 mm in diameter was performed in the parietal bone of skull while keeping the dura mater intact. A cover-glass was placed on

A

Photoactivation

FITC anti-Platelet

Thrombin: 11″ · 43″ · 174″ · 250″

RB: 9″ · 54″ · 214″ · 288″

T+RB: 11″ · 40″ · 119″ · 250″

B

p=0.0002

Average intensity (a.u./pixel): 300 / 250 / 200 / 150 / 100 / 0

RB · T+RB

C

FITC-Fibrinogen

Photoactivation · Off

Thrombin: 5″ · 20″ · 46″

RB: 8″ · 24″ · 43″

T+RB: 6″ · 32″ · 49″

Figure 2. RB- and thrombin/RB-induced photothrombosis manifest divergent patterns of platelet aggregation and fibrin(ogen) extension. (A) Using DyLight488-conjugated anti-GPIbβ antibody to label platelets, intravital microscopy showed the lack of platelet aggregation after systemic intravenous injection of 80 U/kg thrombin and laser photoactivation (supplemental Video 2; n = 3). In contrast, photoactivation after intravenous injection of RB (50 mg/kg) or thrombin/RB (T+RB) induced platelet aggregates of different compactness (see also supplemental Videos 3 and 4, respectively). Arrows indicate the site of photoactivation. (B) Imaging analysis showed a lower average intensity of anti-GPIbβ/platelet fluorescence signals in the T+RB clots (n = 33 in 8 mice) than in RB photothrombosis clots (n = 31 in 6 mice; P = .0002 by unpaired Student t test). (C) Intravital microscopy of FITC-conjugated fibrinogen showed the lack of fibrin(ogen) extension after photoactivation in thrombin-alone injection (supplemental Video 5) and restricted fibrin(ogen) deposits after RB photothrombosis (supplemental Video 6), in contrast to appreciable expansion of fibrin(ogen) deposits in T+RB photothrombosis (supplemental Video 7; n = 3 for each group). Scale bars, 50 μm.

the cranial window, and the cerebral vessels and MCA in the temporal cortex became visible under 20× water-immersion lens. Circulating platelets labeled by DyLight488-conjugated anti-GPIbβ antibody (0.1 mg/kg; Emfret Analytics) or the exogenous fluorescein isothiocyanate (FITC)-Fibrinogen (2 mg/kg; Molecular Innovations) was injected via tail vein 5 minutes before intravital microscopy imaging. Photoactivation on randomly selected cerebral vessels or distal MCA branches (40~60 μm diameter) was induced using a 561-nm laser system (89 North, 10~20 μm diameter) either with (for anti-platelet imaging) or without (for FITC-fibrinogen imaging) neutral density filter. The average fluorescence intensity of platelet was analyzed and quantified using the MetaMorph software (Molecular Devices).

Laser speckle contrast imaging

Cerebral blood flow (CBF) was monitored using a MoorFLPI-2 system (Moor Instruments), as described.[20,21] CBF was measured in both hemispheres (area size for CBF quantification: 3 mm × 4.8 mm) for at least 5 minutes at the designated points after photoactivation or recorded for 70 minutes to assess the responses to tPA-lytic treatment (area size for CBF quantification: 1.6 mm × 1.6 mm). The CBF is shown using a 16-color palette of perfusion units, and quantified as the percentage to the contralateral corresponding region.

Immunohistochemistry and immunoblot

Immunohistochemistry and immunoblotting were performed as previously described.[20-22] The antibodies were rabbit anti-fibrinogen (#MBS315814, MyBioSource), rat anti-TER119 (#14-59-2182, Invitrogen), rat anti-glycoprotein IIb (#553847, Becton Dickinson), Isolectin GS-IB4 (I21413, Invitrogen), and mouse anti-GAPDH (#G8795, Sigma).

Assessment of intracerebral hemorrhage

Intracerebral hemorrhage was quantified using a spectrophotometric assay, as previously described.[23] Briefly, mice were transcardially perfused with phosphate-buffered saline, and the ipsilateral hemisphere was homogenized in 500 μL phosphate-buffered saline containing 0.5% triton X-100, followed by 13 000g centrifuged for 30 minutes. The 200-μL aliquots of supernatant mixed with 800 μL of Drabkin's reagent (Sigma-Aldrich) were reacted at room temperature for 15 minutes and subjected to duplicate measurement of absorbance at 540 nm, using a spectrophotometer (SpectraMax M3, Molecular Device). The standard curve was

Figure 3. T+RB-PTS produces a greater fibrin content in the ensuing clots than RB-PTS. (A) A similar size of infarction was induced by RB (14.4 ± 2.50 mm³; n = 7) or Thrombin-RB (T+RB) photothrombosis (14.1 ± 2.84 mm³; n = 8), whereas photoactivation after systemic intravenous application of thrombin failed to induce cerebral infarct (n = 6). (B-C) Histological analysis of MCA showed a higher content of fibrin (green colored) in blood clots after T+RB photothrombosis than RB photothrombosis, as shown by co-immunostaining of fibrin(ogen)/CD41 (platelets; B), and fibrin/TER119 (RBCs; C) (n = 3 for each group). The transverse sections of MCA (bottom rows) were costained with isolection-B4 (IB4) to outline the vascular lumen. Note the occlusion of the whole vessel, similar to the $FeCl_3$-induced stroke model.[30] Scale bars, 50 μm. (D) Immunoblot analysis indicated greater fibrin deposits in the ipsilateral hemisphere at 2 hours after the T+RB than the RB photothrombosis stroke model. Two representative samples are shown here, as well as the quantification of 3 mice for each model ($P = .027$ by unpaired Student t test). Cont, contralateral hemisphere; Ipsi, ipsilateral hemisphere; UN, uninjured sham mice.
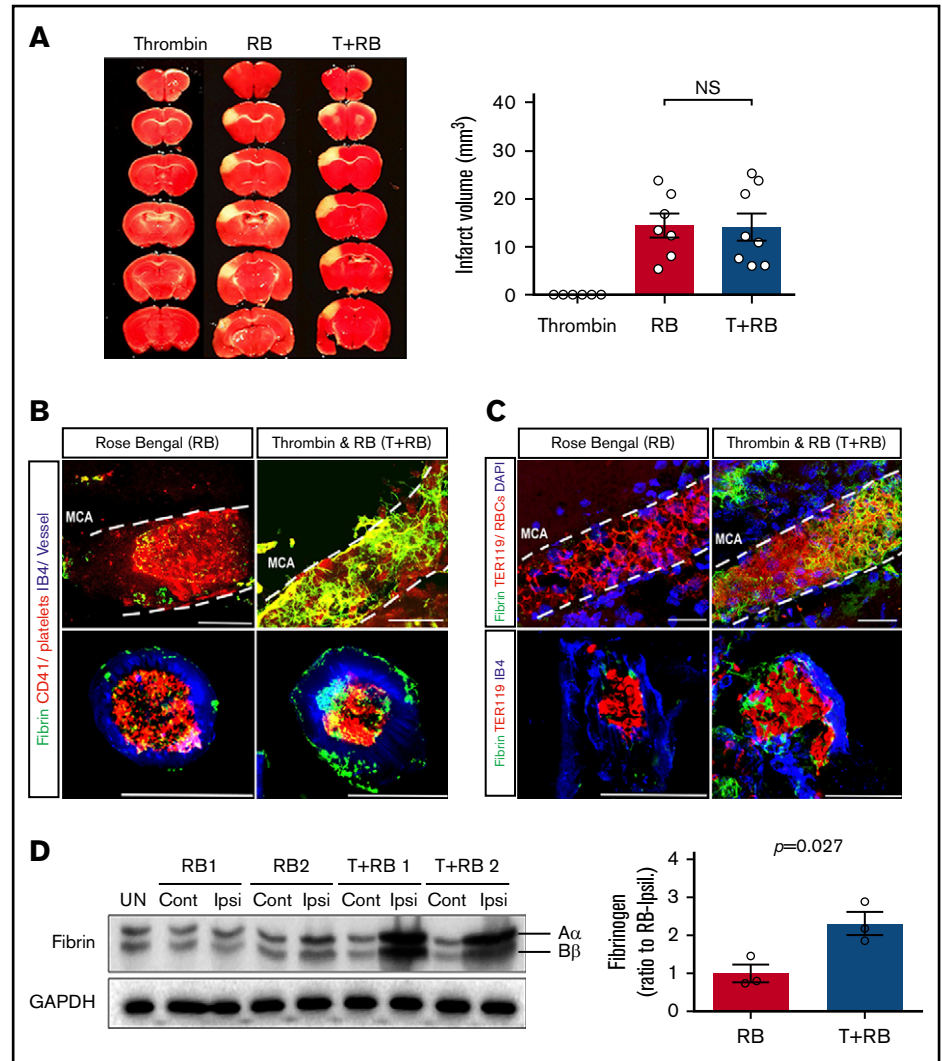
prepared by adding incremental volume of homologous blood (0, 2, 4, 8, 16 μL) into each hemispheric sample from sham mice. Measurements from experimental samples were compared with this standard curve to calculate the hemorrhage volumes in microliters.

Statistical analysis

The Kolmogorov-Smirnov normality test was performed to confirm that the data follows a normal distribution. Statistical analysis was performed using 1-way analysis of variance followed by the posttest of Tukey or unpaired Student t test for 2 groups. $P < .05$ was considered a significant difference. Values were expressed as mean ± standard error of mean.

Results

RB-PTS promotes platelet aggregates that are resistant to tPA-lytic treatment

DyLight488-conjugated anti-GPIbβ antibody was used to visualize the responses of platelets in single small vessel (~50 μm diameter)–targeted RB photothrombosis by intravital microscopy imaging. It was found that the platelets initially formed small clots

along the endothelial wall, but were repeatedly flushed away into the bloodstream (unstable clots). After approximately 150 seconds of photoactivation, the platelet clot became adherent to the endothelium and expanded rapidly in size (stable clots; Figure 1A-B; supplemental Video 1). This pattern of biphasic platelet aggregation differs from those after laser-induced endothelium injury[24] and suggests that platelet activation may be the initiating trigger in RB photothrombosis. We then examined the responses of MCA-targeted RB-PTS to acute tPA treatment (10 mg/kg, 50% as a bolus and 50% infused via tail vein at 30 minutes postphotoactivation) and found no reduction of the infarct size (Figure 1C; $P > .05$ by unpaired Student t test). These results suggest that the clots in RB-PTS are rather resistant to tPA-mediated lytic treatment, similar to the findings in previous studies.[6]

T+RB-PTS produces less-compacted platelet aggregates with a higher fibrin content and greater responsiveness to tPA-lytic treatment

We then used intravital microscopy to compare the responses of platelets to intravenous injection of 80 U/kg thrombin, 50 mg/kg RB,
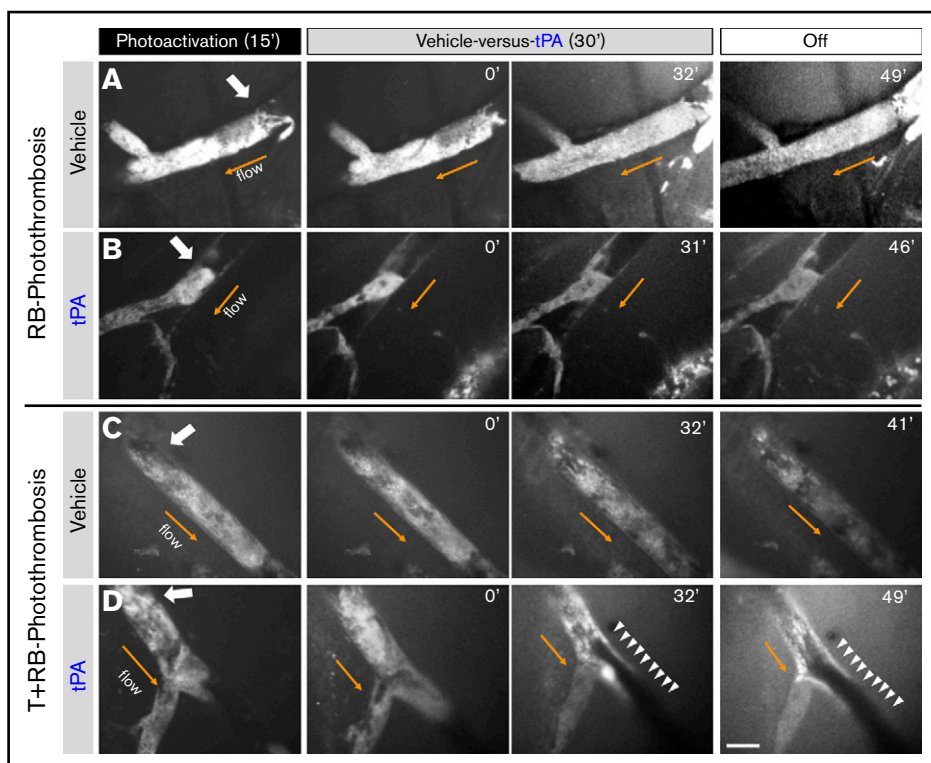
Figure 4. T+RB-PTS is markedly more sensitive to tPA-lytic treatment than RB-PTS. (A-B) Intravital microscopy imaging with DyLight488-conjugated anti-GPIbβ/platelet antibody was used to visualize the clot behaviors during and after vehicle-vs-tPA (10 mg/kg) infusion in single-vessel RB photothrombosis model. Shown are the representative images of the RB clot with the vehicle (A; see also supplemental Video 8; n = 3) or tPA infusion (B; supplemental Video 9; n = 4). Neither tPA or vehicle induced obvious re-canalization in the RB photothrombosis model. White arrow indicates the site of photoactivation (20 μm in diameter). Orange arrow indicates the direction of ar-terial blood flow. (C-D) The same intravital imaging method was used to compare the clot responses to vehicle-vs-tPA (10 mg/kg) infusion after T+RB photo-thrombosis. The vehicle treatment failed to restore the blood flow (C; supplemental Video 10; n = 3), whereas every tPA-treated mouse manifested re-canalization of the occluded artery (arrowheads in D; supplemental Video 11; n = 5). Scale bar, 50 μm.

or the combination of both, in single small vessel photoactivation (Figure 2A). It was found that thrombin photoactivation failed to trigger platelet aggregates (supplemental Video 2), whereas RB photoactivation induced more densely packed platelet aggregates (supplemental Video 3) than T+RB photothrombo-sis (supplemental Video 4). This finding was corroborated by quantification of the anti-GPIbβ immunofluorescence intensity in the RB-vs-T+RB blood clots (Figure 2B; $P = .0002$ by unpaired Student t test). Further, intravital imaging of FITC-conjugated fibrinogen also showed divergent responses to photoactivation by these 3 conditions (Figure 2C). It was evident that systemic intravenous thrombin injection plus photoactivation failed to induce fibrin clots (supplemental Video 5). RB photoactivation led to localized FITC-fibrin clots (supplemental Video 6), but only T+RB photothrombosis resulted in appreciable expansion of the FITC-fibrin clot (supplemental Video 7).

We also compared the responses of thrombin, RB, and combined thrombin/RB to the MCA-targeted photothrombosis. When photo-activation was directed at the proximal MCA branch, systemic intravenous thrombin injection failed to induce infarction, whereas RB and T+RB injection led to a similar size of infarction in the MCA-supplying territory (Figure 3A). Immunostaining of longitu-dinal and transverse sections of clotted blood vessels both revealed mixed fibrin:platelet thrombi in the T+RB stroke model (right panels in Figure 3B-C), but not in the RB model (left panels in Figure 3B-C). Immunoblotting corroborated the finding of more fibrin deposits in ipsilateral hemisphere in T+RB photothrombo-sis than in unchallenged or the RB-photoactivated counterparts (Figure 3D).

We then compared the responses of RB-vs-T+RB photothrombo-sis to intravenous infusion of vehicle or tPA (10 mg/kg, 30 minutes) via intravital imaging. This analysis showed that neither vehicle nor tPA treatment elicited clear recanalization in RB photo-thrombosis (Figure 4A-B; supplemental Videos 8 and 9, respectively). In contrast, intravenous infusion of tPA reliably induced recanalization and restored the blood flow after T+RB photothrombosis (arrowheads in Figure 4D; supple-mental Video 11), whereas vehicle treatment lacked this effect (supplemental Video 10). Together, these results suggest that T+RB photothrombosis produces more balanced fibrin:plate-let clots and greater responses to tPA-lytic treatment than RB-only photothrombosis.

T+RB-PTS is sensitive to tPA-mediated vascular recanalization, CBF improvement, and reduction of the infarct size

Next, we used laser speckle contrast imaging (LSCI) to compare the dynamics of CBF alterations after RB-vs-T+RB photothrombosis targeting proximal MCA branch and the responses to intravenous tPA at the bilateral hemispheric level. A recent study reported progressive increase of the peripheral CBF without recanalization of the clotted proximal MCA from 6 to 120 hours after RB photothrombosis, likely because of ischemia-induced collateral circulation.[5,16-18] Consistent with this report,[5] our results showed that the cortical blood flow dropped to ~35% at 5 hours, but steadily recovered to ~80% from the peripheral to the ischemic core at 7 days postinfarct in both RB and T+RB models (Figure 5A-B). These results suggest the lack of spontaneous large
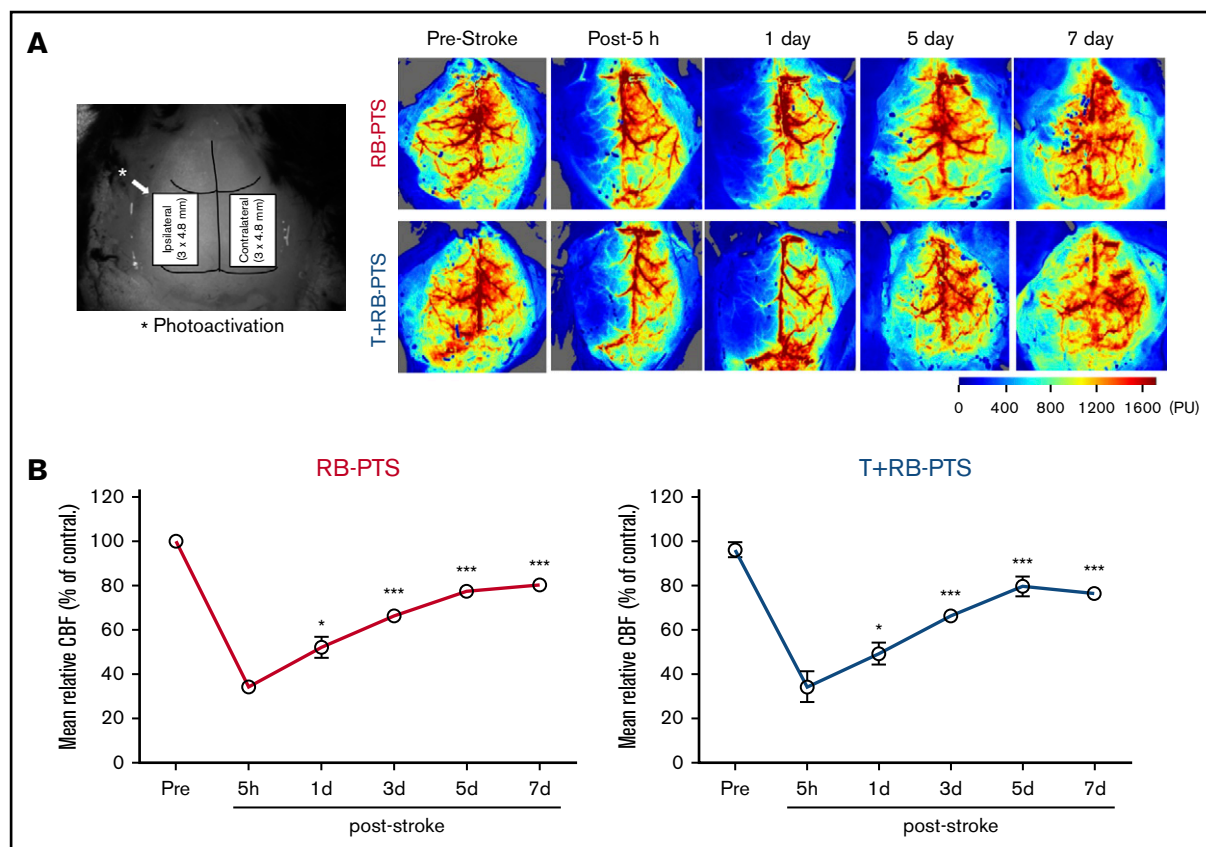
Figure 5. LSCI showed gradual recovery of blood flow in the peripheral ischemic area from 1 day after RB-PTS or T+RB-PTS. (A) The CBF was sequentially measured by LSCI before and after photothrombosis plus ligation of the ipsilateral common carotid artery (from 5 hours to 7 days postphotoactivation), and quantified as the percentage to contralateral hemisphere at each time. Shown are the representative LSCI images at various points after RB-PTS and T+RB-PTS (n = 7 for each group). Also shown are the MCA-suppling territory for CBF measurement (3 mm × 4.8 mm) in both hemispheres. Asterisk indicates the site of proximal MCA-directed photoactivation (1 mm in diameter). Arrow indicates the direction of MCA blood flow. (B) The blood flow in the ipsilateral MCA-supplying territory dropped at 5 hours after photoactivation, but steadily recovered to ~50% at 1 day (*$P <$ .05 compared with the 5-hour postphotoactivation value by 1-way analysis of variance), ~65% at 3 days (***$P <$ .001 compared with the 5-hour value by 1-way analysis of variance), and ~80% at both 5 and 7 days (***) in both RB-PTS and T+RB-PTS models (n = 7 in each group).

artery recanalization after the T+RB photothrombotic stroke model.

We then compared the CBF responses to acute tPA treatment (10 mg/kg; initiated at 30 minutes after photoactivation) by RB-vs-T+RB photothrombosis (Figure 6A). Although the tPA treatment failed to improve CBF in either the proximal or distal MCA-supplying region (areas 1 and 2, respectively) after RB-PTS, it produced step-wise elevation of cortical blood flow in the distal MCA territory (area 2) after T+RB photothrombosis. We also compared CBF at 5 and 24 hours after tPA treatment, and found that tPA produced markedly improved CBF at 24 hours after T+RB-PTS, but failed to elicit significant CBF recovery after RB-PTS (Figure 6B).
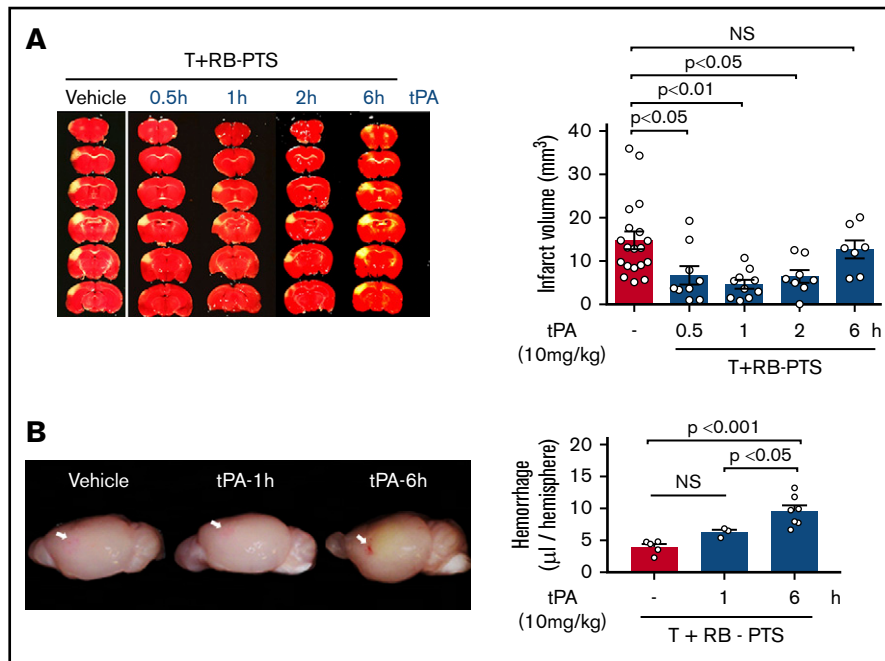
Finally, we examined the effects of reducing the infarct size by tPA-lytic treatment and its therapeutic window in T+RB photothrombosis. Consistent with tPA-mediated CBF recovery, the T+RB PTS model showed significant reduction of the infarct size when the tPA treatment (10 mg/kg) was initiated at 0.5, 1, or 2 hours after photoactivation compared with the vehicle-treated mice, but lost the

benefit if tPA was administered at 6 hours postphotoactivation (Figure 7A). Instead, this delayed tPA treatment led to greater intracerebral hemorrhage at 24 hours postphotoactivation in T+RB photothrombosis (Figure 7B), although the severity of tPA-induced hemorrhage appears milder than in the intraluminal suture MCA occlusion model.[23] Together, these results suggest improved sensitivity to tPA treatment by the modified photothrombotic stroke model.

Discussion

Thromboembolic stroke models are important tools for thrombolytic research, in contrast to the mechanical vascular occlusion models (eg, intraluminal suture MCA occlusion) that produces overly fast reperfusion without obvious blood clots.[25] The advances of endovascular therapies in ischemic stroke have enabled histological analysis of the clinical thrombi to guide the selection of thromboembolic models. These histopathological studies indicated a predominant feature of random fibrin:platelet deposits interspersed with leukocytes and erythrocyte-rich regions.[7,8] In

Figure 6. T+RB-PTS shows better recovery of CBF after tPA-lytic treatment than RB-PTS. (A) Comparison of CBF responses to 10 mg/kg tPA treatment at 30 minutes after photoactivation by LSCI in the proximal MCA-directed RB (n = 4) vs T+RB (n = 3) PTS (asterisk indicates the photoactivation site; white arrow indicates the direction of MCA blood flow). Shown are the typical CBF-tracing and LSCI images of blood flow in the proximal MCA-supplying territory (1), the distal MCA territory (2), and the contralateral hemisphere (3; area size: 1.6 mm × 1.6 mm for each). Note the stepwise CBF elevation in the distal, but not the proximal, MCA territory, in the T+RB-PTS model after tPA infusion. In contrast, the tPA treatment failed to produce CBF recovery in the RB-PTS model. (B) Comparison of CBF recovery at 5 and 24 hours after tPA infusion at 30 minutes postphotoactivation in the RB-PTS and T+RB-PTS model (the area size for LSCI measurement: 3 mm × 4.8 mm). The tPA treatment failed to improve CBF recovery compared with the infusion of vehicle at 5 or 24 hours postphotoactivation (n = 4). In contrast, the same tPA treatment produced ~14% more CBF recovery at 5 hours (P = .13) and ~25% more at 24 hours in the T+RB-PTS model (P = .03; n = 6).

addition, cardioembolic thrombi consist of higher fibrin proportions and more leukocytes than noncardioembolic thrombi.[26] However, contrary to the histological features of clinical thrombi, the standard photothrombosis and $FeCl_3$ stroke models mainly induce platelet aggregates without significant fibrin, whereas in situ MCA microinjection of thrombin induces fibrin polymerization with a low number of cells and platelets.[2,9-12] Here we tested whether the combination of subthreshold thrombin and

Figure 7. Acute infusion of tPA (within 2 hours after photoactivation) reduces the infarct size in T+RB-PTS model. (A) The representative TTC-stained brain slices from mice receiving the vehicle or 10 mg/kg tPA at the indicated time after T+RB-PTS. Quantification showed more than 50% reduction of the infarct size in 0.5-hour tPA-treated (6.7 ± 2.1 mm^3; n = 9; $P < .05$ by 1-way analysis of variance), 1-hour tPA-treated (4.6 ± 1.0 mm^3; n = 10; $P < .01$), and 2-hour tPA-treated (6.4 ± 1.5 mm^3; n = 8; $P < .05$) group, but not in the 6-hour tPA-treated group (15.2 ± 3.1 mm^3; n = 7), compared with the vehicle-treated group (14.8 ± 2 mm^3; n = 19). Normal distribution of the infarct size in each group was ascertained by the Komogorov-Smirnov normality test. (B) The representative images of brain surface in mice treated by vehicle, 1-hour tPA, or 6-hour PA at 24 hours after T+RB-PTS. Note the more pronounced hemorrhage spot (indicated by arrow) in the MCA-supplying territory in the mice that received the delayed, 6-hour tPA treatment. Quantification of cerebral hemorrhage indicated a higher content of hemoglobin in 6-hour tPA photothrombosis (9.6 ± 0.9 μL; n = 7) than in the vehicle (4.0 ± 0.5 μL; n = 5) or 1-hour tPA-treated (6.2 ± 0.4 μL; n = 3) groups.

RB for photoactivation produces more balanced platelet:fibrin clots and improved responses to the tPA-lytic treatment. Consistent with our hypothesis, the evidence from intravital imaging, immunostaining, and immunoblotting analysis all supported a greater fibrin content and higher sensitivity to tPA-lytic treatment in the thrombin-RB photothrombotic model. Its therapeutic window for tPA treatment (~2 hours) is similar to that of the thrombin microinjection model (3 hours).[12] Given its more balanced platelet:fibrin clot-composition, the thrombin modified photothrombotic stroke model may be uniquely positioned to study combined fibrinolytic/antiplatelet therapies or head-to-head comparison of tPA-vs-Tenecteplase for thrombolysis.[15]

Our results also revealed differing benefits of tPA-lytic treatment in single small artery-vs-the MCA-targeted photothrombosis. In small artery-targeted thrombin photothrombosis, tPA infusion readily produces vascular recanalization. In contrast, in the proximal MCA-targeted photothrombosis, tPA primarily improves blood flow in the ischemic border without large artery recanalization, which may be partially a result of severe endothelial injury from the photoactivation laser beam, leading to tPA-refractory vascular occlusion. However, because the in situ thrombin microinjection model also responds to the tPA treatment by centripetal retreat of infarct,[6,11] tPA may prevent secondary thrombosis or boost ischemia-induced collateral circulation in the border zone in MCA-targeted

photothrombosis.[5,27] Past studies have reported that both recanalization and collateral circulation predict the ischemic stroke outcomes.[28,29] Hence, the proximal MCA-targeted thrombin photothrombotic stroke model may be also useful to develop novel strategies of improved microcirculation and cortical collateral circulation after the thrombus retrieval treatment.

In conclusion, thrombin-enhanced photothrombosis overcomes critical limitations of the conventional RB-photothrombotic stroke model (ie, platelet-dominant clots with poor responses to tPA-lytic treatment), while retaining its merits in low mortality, relatively simple surgery, plus consistent location and infarct size. As such, the thrombin-enhanced photothrombosis is a worthy addition to the repertoire of preclinical stroke models.

Acknowledgments

Authorship

Contribution: Y.-Y.S., Y.-M.K., and C.-Y.K. designed the study and wrote the manuscript; and Y.-Y.S., Y.-M.K., J.C.S.-M., M.R.S., and H.-R.C. performed the experiments.

Conflict-of-interest disclosure: The authors declare no competing financial

ORCID profiles: Y.-Y.S., 0000-0002-6608-1347; Y.-M.K., 0000-0002-7949-6664.

Correspondence: Chia-Yi Kuan, Department of Neuroscience, University of Virginia School of Medicine, 409 Lane Rd, MR-4, 4046, Charlottesville, VA 22908; e-mail: alex.kuan@virginia.edu.

References

1. Watson BD, Dietrich WD, Busto R, Wachtel MS, Ginsberg MD. Induction of reproducible brain infarction by photochemically initiated thrombosis. *Ann Neurol*. 1985;17(5):497-504.

2. Watson BD, Prado R, Veloso A, Brunschwig JP, Dietrich WD. Cerebral blood flow restoration and reperfusion injury after ultraviolet laser-facilitated middle cerebral artery recanalization in rat thrombotic stroke. *Stroke*. 2002;33(2):428-434.

3. Sommer CJ. Ischemic stroke: experimental models and reality. *Acta Neuropathol*. 2017;133(2):245-261.

4. Uzdensky AB. Photothrombotic Stroke as a Model of Ischemic Stroke. *Transl Stroke Res*. 2018;9(5):437-451.

5. Clark TA, Sullender C, Kazmi SM, et al. Artery targeted photothrombosis widens the vascular penumbra, instigates peri-infarct neovascularization and models forelimb impairments. *Sci Rep*. 2019;9(1):2323.

6. Peña-Martínez C, Durán-Laforet V, García-Culebras A, et al. Pharmacological Modulation of Neutrophil Extracellular Traps Reverses Thrombotic Stroke tPA (Tissue-Type Plasminogen Activator) Resistance. *Stroke*. 2019;50(11):3228-3237.

7. Marder VJ, Chute DJ, Starkman S, et al. Analysis of thrombi retrieved from cerebral arteries of patients with acute ischemic stroke. *Stroke*. 2006;37(8):2086-2093.

8. Bacigaluppi M, Semerano A, Gullotta GS, Strambo D. Insights from thrombi retrieved in stroke due to large vessel occlusion. *J Cereb Blood Flow Metab*. 2019;39(8):1433-1451.

9. Denorme F, Langhauser F, Desender L, et al. ADAMTS13-mediated thrombolysis of t-PA-resistant occlusions in ischemic stroke in mice. *Blood*. 2016;127(19):2337-2345.

10. Martinez de Lizarrondo S, Gakuba C, Herbig BA, et al. Potent Thrombolytic effect of *N*-acetylcysteine on arterial thrombi. *Circulation*. 2017;136(7):646-660.

11. Orset C, Haelewyn B, Allan SM, et al. Efficacy of alteplase in a mouse model of acute ischemic stroke: a retrospective pooled analysis. *Stroke*. 2016;47(5):1312-1318.

12. Orset C, Macrez R, Young AR, et al. Mouse model of in situ thromboembolic stroke and reperfusion. *Stroke*. 2007;38(10):2771-2778.

13. Wyseure T, Rubio M, Denorme F, et al. Innovative thrombolytic strategy using a heterodimer diabody against TAFI and PAI-1 in mouse models of thrombosis and stroke. *Blood*. 2015;125(8):1325-1332.

14. McFadyen JD, Schaff M, Peter K. Current and future antiplatelet therapies: emphasis on preserving haemostasis. *Nat Rev Cardiol*. 2018;15(3):181-191.

15. Coutts SB, Berge E, Campbell BC, Muir KW, Parsons MW. Tenecteplase for the treatment of acute ischemic stroke: A review of completed and ongoing randomized controlled trials. *Int J Stroke*. 2018;13(9):885-892.

16. Bang OY, Goyal M, Liebeskind DS. Collateral circulation in ischemic stroke: assessment tools and therapeutic strategies. *Stroke*. 2015;46(11):3302-3309.

17. Faber JE, Chilian WM, Deindl E, van Royen N, Simons M. A brief etymology of the collateral circulation. *Arterioscler Thromb Vasc Biol*. 2014;34(9):1854-1859.

18. Piedade GS, Schirmer CM, Goren O, et al. Cerebral collateral circulation: a review in the context of ischemic stroke and mechanical thrombectomy. *World Neurosurg*. 2019;122:33-42.

19. Su EJ, Fredriksson L, Geyer M, et al. Activation of PDGF-CC by tissue plasminogen activator impairs blood-brain barrier integrity during ischemic stroke. *Nat Med*. 2008;14(7):731-737.

20. Sun YY, Morozov YM, Yang D, et al. Synergy of combined tPA-edaravone therapy in experimental thrombotic stroke. *PLoS One*. 2014;9(6):e98807.

21. Sun YY, Li Y, Wali B, et al. Prophylactic edaravone prevents transient hypoxic-ischemic brain injury: implications for perioperative neuroprotection. *Stroke*. 2015;46(7):1947-1955.

22. Sun YY, Lee J, Huang H, et al. Sickle mice are sensitive to hypoxia/ischemia-induced stroke but respond to tissue-type plasminogen activator treatment. *Stroke*. 2017;48(12):3347-3355.

23. Mao L, Li P, Zhu W, et al. Regulatory T cells ameliorate tissue plasminogen activator-induced brain haemorrhage after stroke. *Brain*. 2017;140(7):1914-1931.

24. Falati S, Gross P, Merrill-Skoloff G, Furie BC, Furie B. Real-time in vivo imaging of platelets, tissue factor and fibrin during arterial thrombus formation in the mouse. *Nat Med*. 2002;8(10):1175-1181.

25. Hossmann KA. The two pathophysiologies of focal brain ischemia: implications for translational stroke research. *J Cereb Blood Flow Metab*. 2012;32(7):1310-1316.

26. Sporns PB, Hanning U, Schwindt W, et al. Ischemic stroke: what does the histological composition tell us about the origin of the thrombus? *Stroke*. 2017;48(8):2206-2210.

27. Akamatsu Y, Nishijima Y, Lee CC, et al. Impaired leptomeningeal collateral flow contributes to the poor outcome following experimental stroke in the Type 2 diabetic mice. *J Neurosci.* 2015;35(9):3851-3864.

28. Rha JH, Saver JL. The impact of recanalization on ischemic stroke outcome: a meta-analysis. *Stroke.* 2007;38(3):967-973.

29. Maas MB, Lev MH, Ay H, et al. Collateral vessels on CT angiography predict outcome in acute ischemic stroke. *Stroke.* 2009;40(9):3001-3005.

30. Le Behot A, Gauberti M, Martinez De Lizarrondo S, et al. GpIbα-VWF blockade restores vessel patency by dissolving platelet aggregates formed under very high shear rate in mice. *Blood.* 2014;123(21):3354-3363.